THE JOURNAL OF BIOLOGICAL CHEMISTRY VOL. 283, NO. 43, pp. 28873–28880, October 24, 2008

Irreversible Oxidation of the Active-site Cysteine of Peroxiredoxin to Cysteine Sulfonic Acid for Enhanced Molecular Chaperone Activity*

Received for publication, May 29, 2008, and in revised form, August 13, 2008 Published, JBC Papers in Press, August 25, 2008, DOI 10.1074/jbc.M804087200

Jung Chae Lim[‡], Hoon-In Choi[‡], Yu Sun Park[‡], Hyung Wook Nam[§], Hyun Ae Woo[¶], Ki-Sun Kwon[‖], Yu Sam Kim[§], Sue Goo Rhee[¶], Kanghwa Kim[**], and Ho Zoon Chae[‡ ‡‡1]

From the Departments of [‡]Biological Sciences and [**]Food and Nutrition and the [‡‡]School of Biological Sciences and Technology, Chonnam National University, Gwangju 500-757, Korea, the [§]Department of Biochemistry, College of Science, Protein Network Research Center, Yonsei University, Seoul 120-749, Korea, the [¶]Division of Life and Pharmaceutical Sciences, Ewha Womans University, Seoul 120-750, Korea, and the [‖]Korea Laboratory of Cell Signaling, Omics and Integration Research Center, Korea Research Institute of Bioscience and Biotechnology, Daejeon 305-333, Korea

The thiol (–SH) of the active cysteine residue in peroxiredoxin (Prx) is known to be reversibly hyperoxidized to cysteine sulfinic acid ($–SO_2H$), which can be reduced back to thiol by sulfiredoxin/sestrin. However, hyperoxidized Prx of an irreversible nature has not been reported yet. Using an antibody developed against the sulfonylated ($–SO_3H$) yeast Prx (Tsa1p) active-site peptide (AFTFVCPTEI), we observed an increase in the immunoblot intensity in proportion to the H_2O_2 concentrations administered to the yeast cells. We identified two species of hyperoxidized Tsa1p: one can be reduced back (reversible) with sulfiredoxin, and the other cannot (irreversible). Irreversibly hyperoxidized Tsa1p was identified as containing the active-site cysteine sulfonic acid (Tsa1p-SO_3H) by mass spectrometry. Tsa1p-SO_3H was not an autoxidation product of Tsa1p-SO_2H and was maintained in yeast cells even after two doubling cycles. Tsa1p-SO_3H self-assembled into a ring-shaped multimeric form was shown by electron microscopy. Although the Tsa1p-SO_3H multimer lost its peroxidase activity, it gained ~4-fold higher chaperone activity compared with Tsa1p-SH. In this study, we identify an irreversibly hyperoxidized Prx, Tsa1p-SO_3H, with enhanced molecular chaperone activity and suggest that Tsa1p-SO_3H is a marker of cumulative oxidative stress in cells.

Thiols of cysteine residues in proteins are some of the most vulnerable targets of peroxide in cells, and based on their sensitivity to peroxide, thiol groups have been employed as redox sensors in biological systems (1–4). The reaction of cysteinyl thiolates with hydrogen peroxide results in the formation of different oxidation forms, such as sulfenic acid (–SOH), sulfinic acid ($–SO_2H$), sulfonic acid ($–SO_3H$), and disulfide (–S-S–), including glutathione *S*-conjugate and disulfide *S*-oxides (5–8). A typical reaction mechanism of cysteine-based peroxide reductases, such as 2-Cys peroxiredoxins (Prxs),[2] includes the oxidation of an active-site thiolate to sulfenic acid by accepting an oxygen atom from peroxide, resolution by a nearby cysteine residue to form a disulfide bond, and final reduction to thiolates sequentially (9–12). Hyperoxidation of the peroxidatic cysteine (C_P) of Prx to cysteine sulfinic or cysteine sulfonic acid can occur both under normal culture conditions and under oxidative stress (13–16). During normal peroxidase catalysis of human Prx I with a low and steady concentration of H_2O_2 (<1 μM), 0.072% of the C_P thiolate hyperoxidizes to cysteine sulfinic acid per turnover (17). Hyperoxidation of a cysteine residue to cysteine sulfinic acid alters the structure and the catalytic activities of various proteins, such as Prxs, MMP-7 (matrix metalloproteinase-7) (18), glyceraldehyde-3-phosphate dehydrogenase (14), DJ-1 (20), carbonic anhydrase III (21), MKP3 (mitogen-activated protein kinase phosphatase-3) (22), and PTP-1B (protein-tyrosine phosphatase-1B) (23, 24). Cysteine sulfinylation in proteins has been recognized as a process of losing biological function, but it is now seen as a precise cellular regulation mechanism after the identification of the sulfiredoxin/sestrin-mediated retroreduction, which reverses cysteine sulfinic acid (Cys-SO_2H) to sulfhydryl (Cys-SH), and the identification of the novel functions of sulfinylated proteins (8, 25–28, 30–34). Sulfinyl hyperoxidation induces a functional switch of human Prx II, a 2-Cys Prx, from a cellular peroxidase to a molecular chaperone (32, 33). Temporal sulfinylation of Tsa1p, a yeast 2-Cys Prx, negatively regulates the Tsa1p-Pap1p redox relay (30). Reversible sulfinylation of human Prx II with an accompanying structural transition to large filamentous oligomeric forms regulates hydrogen peroxide-dependent cell cycle arrest and release (34).

In contrast to the reversibly hyperoxidized Cys-SO_2H in proteins, irreversibly hyperoxidized Cys-SO_3H is generally believed to be an impaired dead end product, which is destined to be removed (35, 36). The sulfonic acid state of hyperoxidized C_P of mammalian 2-Cys Prx proteins, such as human Prxs II and III, was observed by in-gel tryptic digestion followed by

* This work was supported by Korea Research Foundation Grant KRF-2007-0940 and Korea Science and Engineering Foundation Grant RO1-2004-000-10242-0 (to H. Z. C.) and Korean Ministry of Science and Technology Grants M10642040003 and M10648000164 (to K.-S. K.). The costs of publication of this article were defrayed in part by the payment of page charges. This article must therefore be hereby marked "*advertisement*" in accordance with 18 U.S.C. Section 1734 solely to indicate this fact.

[1] To whom correspondence should be addressed. Tel.: 82-62-530-3398; Fax: 82-62-530-2199; E-mail: hzchae@jnu.ac.kr.

[2] The abbreviations used are: Prx, peroxiredoxin; C_P, peroxidatic cysteine; SD, synthetic defined; Trx, thioredoxin; DTT, dithiothreitol; Srx1, sulfiredoxin 1; CHAPS, 3-[(3-cholamidopropyl)dimethylammonio]-1-propanesulfonic acid.

mass spectrometric analysis (15). Later, it was proven that sulfonylation of C_P occurs as a result of air oxidation from cysteine sulfinic acid during protease treatment for peptide fingerprinting under denaturing conditions (17). To date, there is no known systematic study examining the conditions of irreversible hyperoxidation or switching of enzyme activity by irreversibly hyperoxidized cysteine residues. Here, we report the hyperoxidation of the active-site Cys-SH to Cys-SO_3H in Tsa1p, the reaction that induces activity switching from a peroxidase to an enhanced molecular chaperone. In addition, we also demonstrate the maintenance of Tsa1p-SO_3H in yeast cells and the possibility of hyperoxidation systems that facilitate the irreversible hyperoxidation of Tsa1p in yeast cells.

EXPERIMENTAL PROCEDURES

Preparation of Antibodies Specific for Sulfonylated Tsa1p—A peptide (AFTFVCPTEI) that corresponds to the active site of yeast Tsa1p was oxidized by performic acid, conjugated to keyhole limpet hemocyanin (Pierce), and used to generate rabbit antibodies as described previously (38).

Hyperoxidation and Retroreduction of Tsa1p in Yeast Cells and in Vitro—The *Saccharomyces cerevisiae* wild-type strain S288C was used in this experiment. Yeast cells were grown overnight at 30 °C in YPD medium (1% yeast extract, 2% Bactopeptone, and 2% glucose) and then transferred to synthetic defined (SD) medium (0.67% yeast nitrogen base and 2% glucose). For hyperoxidation, log-phase cells (A_{600} = 0.5) were exposed to various concentrations of H_2O_2 for 10 min and harvested. For retroreduction of Tsa1p in yeast cells, after a 10-min exposure to H_2O_2, yeast cells were allowed to recover in fresh SD medium for 3 h at 30 °C in the presence of cycloheximide (50 μg/ml). Collected cells were disrupted by glass beads using a minibead beater (BioSpec Products, Inc.) in lysis buffer (50 mM Tris-HCl (pH 7.5), 1 mM EDTA, and 1 mM phenylmethylsulfonyl fluoride), and the crude cell lysates were separated on SDS-polyacrylamide gel or a two-dimensional polyacrylamide gel. Tsa1p was visualized with anti-Tsa1p antiserum regardless of its oxidation state, and the presence of hyperoxidized Tsa1p was verified with anti-Tsa1p-SO_3H antiserum. *In vitro* hyperoxidation of Tsa1p (0.31 μM) was performed in a thioredoxin (Trx)-dependent oxidation mixture containing 50 mM HEPES-NaOH (pH 7.0), 5.95 μM Trx, 0.1 μM Trx reductase, and 0.25 mM NADPH with various H_2O_2 concentrations for 10 min at 30 °C. For retroreduction *in vitro*, hyperoxidized Tsa1p was incubated in retroreduction mixture containing 1.2 μM sulfiredoxin 1 (Srx1), 1 mM ATP, 1 mM $MgCl_2$, and 2.5 mM dithiothreitol (DTT) for 1 h at 30 °C.

Two-dimensional SDS-PAGE—Yeast crude extracts (10 μg) were mixed with rehydration buffer (8 M urea, 2% CHAPS, 0.5% immobilized pH gradient buffer, 20 mM DTT, and 0.005% bromphenol blue) and loaded onto immobilized pH gradient strips (pH 3–10, 13 cm, Amersham Biosciences). Isoelectric focusing was performed with an IPGphor isoelectric focusing unit (Amersham Biosciences) according to the instruction manual. After reduction and alkylation, second dimension electrophoresis was conducted on a 12% SDS-polyacrylamide gel using an SE600 vertical unit (Amersham Biosciences). Proteins from the SDS-polyacrylamide gel were electrophoretically transferred onto nitrocellulose membrane. Tsa1p was probed on the membrane with anti-Tsa1p or anti-Tsa1p-SO_3H antiserum, and the immune complexes were visualized with alkaline phosphatase-conjugated secondary antibodies using nitro blue tetrazolium and 5-bromo-4-chloro-3-indolyl phosphate.

Immunoprecipitation—Yeast cell lysates were prepared with buffer A (50 mM Tris-HCl (pH 8.0), 150 mM NaCl, and 1 mM phenylmethylsulfonyl fluoride), and anti-Tsa1p antibody-conjugated protein G-Sepharose (2 μl of antibody with 30 μl of resin) was equilibrated with buffer B (buffer A containing 0.1% Nonidet P-40). Cell lysates (500 μg/ml protein) were incubated with the resin for 1 h at 4 °C, and the supernatant was then removed by centrifugation. After washing with buffer B, immune complexes were subjected to immunoblot analysis with anti-Srx1 antibody.

Mass Analysis—Mass analysis was performed in parallel on a QSTAR pulsar quadrupole time-of-flight mass spectrometer (Applied Biosystems) equipped with nanoelectrospray ion sources (Protana, Odense, Denmark). The analytes were dissolved in acetonitrile/water (50:50, v/v) and loaded into pre-opened "medium" borosilicate spray capillaries for off-line nanoelectrospray (Proxeon Biosystems, Odense). A potential of 1000 V was applied to the loaded glass capillary tip. Electrospray ionization mass spectra were collected for 1 min, and the masses of proteins were calculated by deconvolving multiple charged ions with m/z values and corresponding total charges using AnalystQS software (Version 1.0, Applied Biosystems).

Size Exclusion Chromatography—Size exclusion chromatography was performed using a TSK-GEL G3000SWXL column (Tosoh). Intact Tsa1p-SH or Tsa1p-SO_3H was injected into the column, which was equilibrated with 50 mM sodium phosphate buffer (pH 7.0) containing 100 mM NaCl at a flow rate of 0.5 ml/min. Determination of molecular masses was referenced against protein standards (Bio-Rad): thyroglobin (670 kDa), bovine γ-globin (158 kDa), ovalbumin (44 kDa), equine myoglobin (17 kDa), and vitamin B_{12} (1.35 kDa).

Electron Microscopy—Transmission electron microscopy analyses were performed at the Korea Basic Science Institute. Proteins were negatively stained with 2% (w/v) uranyl acetate, and transmission electron microscope images were obtained with a Zeiss EM 912 Omega microscope operating at an acceleration voltage of 120 kV.

Trx-dependent Peroxidase Assay and Chaperone Assay—The rate of peroxide reduction was monitored as a decrease in absorbance at 340 nm by NADPH oxidation at 30 °C using a Jasco UV-visible spectrophotometer equipped with a thermostatted cell holder. Reactions were initiated by adding the designated concentrations of hydrogen peroxide in a Trx-dependent oxidation mixture containing 50 mM HEPES-NaOH (pH 7.0), 5.95 μM Trx, 0.1 μM Trx reductase, and 0.25 mM NADPH. Specific activities were calculated from the initial linear portion of the assay. Chaperone activity was measured by its capacity to inhibit thermal aggregation of firefly luciferase (Roche Applied Science). Luciferase (0.15 μM) was incubated with Tsa1p-SH or Tsa1p-SO_3H in 25 mM HEPES-KOH buffer (pH 7.9) at 47 °C for 30 min, and the thermal aggregation of luciferase was monitored by measuring the light scattering at 320 nm.

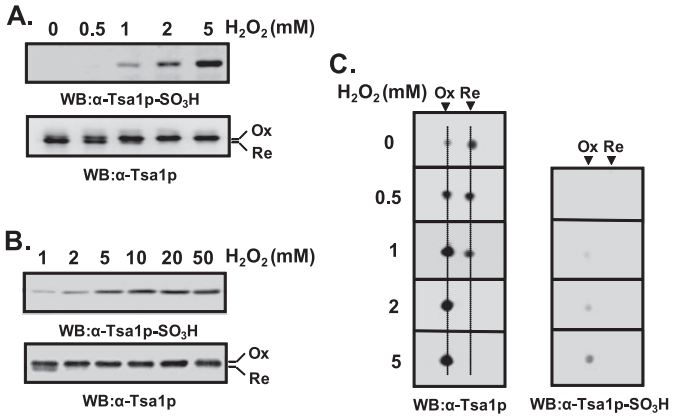

FIGURE 1. **Different reactivity of hyperoxidized Tsa1p with anti-Tsa1p-SO_3H antiserum.** Log-phase yeast cells (A_{600} = 0.5) were exposed to the indicated concentrations of H_2O_2 for 10 min and disrupted in lysis buffer (50 mM Tris-HCl (pH 7.5), 1 mM EDTA, and 1 mM phenylmethylsulfonyl fluoride). Cell lysates were separated by SDS-PAGE (*A* and *B*) or two-dimensional PAGE (*C*) and probed with anti-Tsa1p or anti-Tsa1p-SO_3H antiserum. The positions of hyperoxidized (*Ox*) and reduced (*Re*) forms of Tsa1p are indicated. *WB*, Western blot.

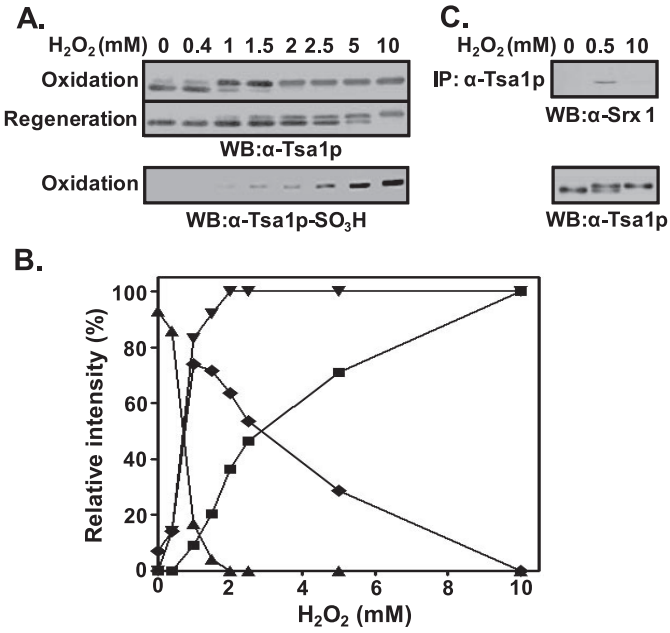

FIGURE 2. **Reversibly and irreversibly hyperoxidized forms of Tsa1p.** *A*, exponentially growing yeast cells (A_{600} = 0.5) were exposed to the indicated concentrations of H_2O_2 for 10 min. For the retroreduction of hyperoxidized Tsa1p, yeast cells were allowed to recover from H_2O_2 stress for 3 h in fresh SD medium in the presence of cycloheximide (50 μg/ml). Redox states of Tsa1p were examined by comparing immune reactivity with anti-Tsa1p and anti-Tsa1p-SO_3H antisera. *WB*, Western blot. *B*, shown is a graphical demonstration of the relative proportions of reduced (▲), hyperoxidized overall (▼), reversibly hyperoxidized (◆), and irreversibly hyperoxidized (■) Tsa1p. The relative intensities of the corresponding bands probed with anti-Tsa1p antibody were quantified by densitometry (Typhoon, GE Healthcare). *C*, immunoprecipitation (*IP*) with anti-Tsa1p antibody was performed using the crude yeast lysates exposed to 0.5 mM (for reversible hyperoxidation) or 10 mM (for irreversible hyperoxidation) hydrogen peroxide for 10 min. Immune complexes were separated on SDS-polyacrylamide gel and visualized with anti-Srx1 antiserum.

RESULTS

Two Different Hyperoxidation States of Tsa1p—Hyperoxidation of C_P residues of Prx proteins to cysteine sulfinic acid (C_P-SO_2H) and the corresponding spot migration on two-dimensional polyacrylamide gels have been studied in both mammalian and yeast cells (15–17). Although an antiserum against mammalian hyperoxidized Prx proteins was developed and characterized, its specificity for two hyperoxidized states, C_P-SO_2H and C_P-SO_3H, needs to be redetermined in detail (38). We also raised rabbit antiserum against the Tsa1p active-site peptide containing C_P-SO_3H following the previous protocol for mammalian anti-Prx-SO_3H antiserum (38). The reactivity of anti-Tsa1p-SO_3H antiserum to yeast cell lysates increased in proportion to hydrogen peroxide concentrations administered to the cells (Fig. 1, *A* and *B*, *upper panels*). By comparing the mobilities of immunoreactive bands to anti-Tsa1p and anti-Tsa1p-SO_3H antisera (Fig. 1, *A* and *B*), we concluded that the hyperoxidized Tsa1p migrated slower than the reduced form on SDS-polyacrylamide gel. However, the extent of intensity increases in anti-Tsa1p-SO_3H-immunoreactive bands upon hydrogen peroxide treatment did not correlate well with that of slow migrating anti-Tsa1p-immunoreactive bands. Although anti-Tsa1p-SO_3H-immunoreactive bands showed linear increases up to 10 mM hydrogen peroxide (Fig. 1, *A* and *B*, *upper panels*), slow migrating anti-Tsa1p-immunoreactive bands showed saturation at 2 mM hydrogen peroxide, suggesting that the latter contains other species (probably Tsa1p-SO_2H) as well as the species reactive to anti-Tsa1p-SO_3H antiserum. Two-dimensional PAGE analysis showed results consistent with those from SDS-PAGE (Fig. 1*C*). With increasing concentrations of hydrogen peroxide administered to the cells, the hyperoxidized Tsa1p spot gained intensity, whereas the reduced Tsa1p spot lost intensity. Consistently, hyperoxidized Tsa1p migrated slower than the reduced form on two-dimensional polyacrylamide gel (Fig. 1*C*, *left panel*). The hyperoxidized spots detected by the two antisera showed different patterns of intensity increases, similar to the results in Fig. 1*A*, also suggesting the existence of different species at the same spot location.

Retroreducibility of the Two Different Hyperoxidized Forms of Tsa1p—The retroreduction of Tsa1p-C_P-SO_2H to Tsa1p-C_P-SH by the catalytic activity of Srx1/sestrin 2 in the presence of ATP and $MgCl_2$ has been reported (25–28). We wondered if the two different hyperoxidized forms of Tsa1p revert to the reduced form (Tsa1p-C_P-SH). When cells were treated with 1 mM hydrogen peroxide, ~78% of the hyperoxidized Tsa1p was retroreduced within 3 h after the removal of peroxide. However, when cells were exposed to 2.5 and 5 mM hydrogen peroxide, 53 and 28% of the Tsa1p were retroreduced, respectively. Treatment with 10 mM hydrogen peroxide totally disabled retroreduction. Based on these results, high doses of hydrogen peroxide seem to make irreversibly oxidized products. Subtraction of reversibly oxidized products (fast migrating bands) (Fig. 2*A*, *middle panel*) from the total oxidized product (slow migrating bands) (*upper panel*) can yield irreversibly oxidized products (*lower panel*), presented in Fig. 2*B*. As expected, irreversibly hyperoxidized Tsa1p obtained by treatment with 10 mM hydrogen peroxide failed to associate with Srx1, whereas reversibly hyperoxidized Tsa1p obtained by treatment with 0.5 mM hydrogen peroxide associated with Srx1 (Fig. 2*C*). These results support the presence of irreversibly hyperoxidized Tsa1p, which is reactive to anti-Tsa1p-SO_3H antiserum.

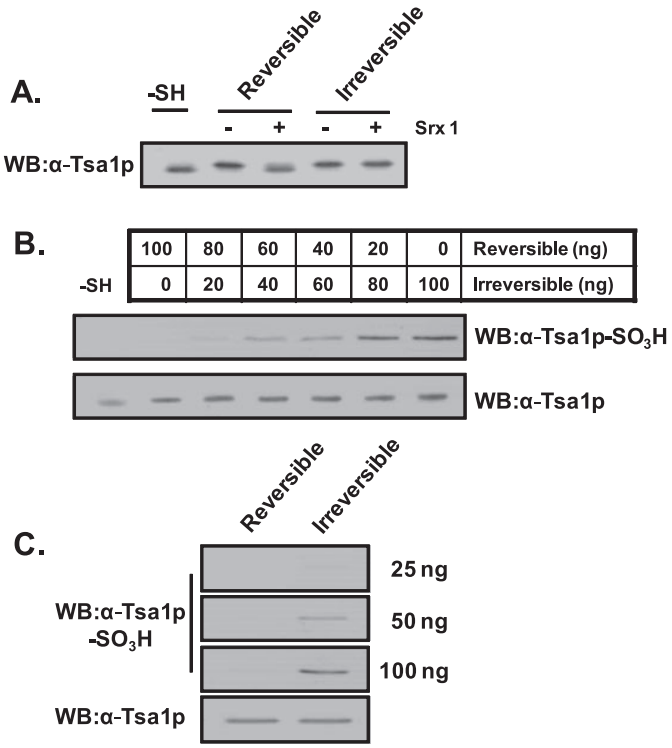

FIGURE 3. **Specificity of anti-Tsa1p-SO_3H antiserum for reversibly and irreversibly hyperoxidized Tsa1p.** Purified Tsa1p-SH (0.3 μM) was incubated in a 150-μl reaction mixture containing 50 mM HEPES-NaOH (pH 7.0), 5.95 μM Trx, 0.1 μM Trx reductase, 0.25 mM NADPH, and 0.2 or 50 mM H_2O_2 for reversible or irreversible hyperoxidation of Tsa1p, respectively (*A*). The hyperoxidation reaction was performed for 10 min at 30 °C. The retroreducibility of hyperoxidized Tsa1p was determined by reaction with 1.2 μM Srx1, 1 mM ATP, 1 mM $MgCl_2$, and 2.5 mM DTT for 1 h at 30 °C. The reaction specificity of anti-Tsa1p-SO_3H antiserum was examined in the mixture of reversibly and irreversibly hyperoxidized Tsa1p in the indicated ratios to yield a total of 100 ng of Tsa1p (*B*) and in the same amount of the two oxidized forms (*C*). *WB*, Western blot.

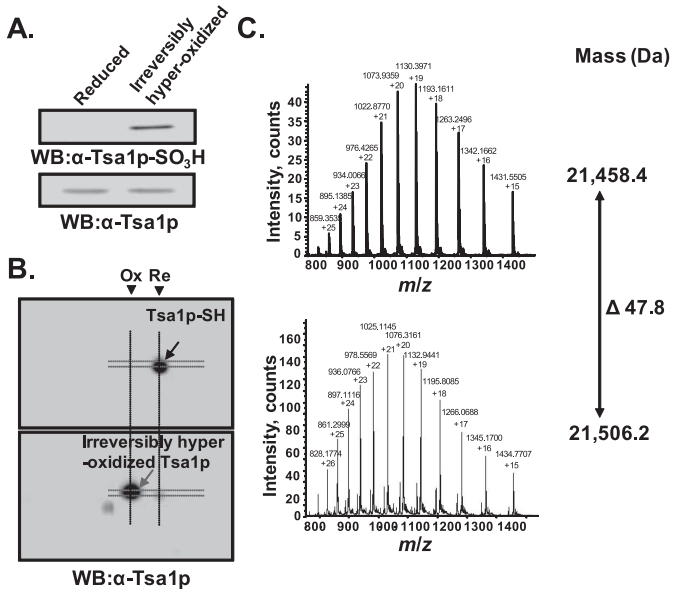

FIGURE 4. **Mass analysis of irreversibly hyperoxidized Tsa1p.** Tsa1p-SH and irreversibly hyperoxidized Tsa1p were purified from yeast cells before and after treatment with 10 mM H_2O_2. *A* and *B*, the redox states of purified Tsa1p were analyzed by SDS-PAGE and two-dimensional PAGE analyses. Bands or spots were visualized with anti-Tsa1p or anti-Tsa1p-SO_3H antiserum. *WB*, Western blot; *Ox*, hyperoxidized Tsa1p; *Re*, reduced Tsa1p. *C*, the masses of Tsa1p-SH (*upper panel*) and irreversibly hyperoxidized Tsa1p (*lower panel*) were determined using a QSTAR pulsar quadrupole time-of-flight mass spectrometer equipped with nanoelectrospray ion sources.

Specificity of Anti-Tsa1p-SO_3H Antiserum for Irreversibly Hyperoxidized Tsa1p—Purified Tsa1p was treated with 0.2 and 50 mM hydrogen peroxide to prepare reversibly and irreversibly hyperoxidized Tsa1p. The reversibility was determined by retroreduction assay with Srx1 (Fig. 3*A*). Both species were mixed in different ratios and probed with anti-Tsa1p-SO_3H antiserum after separation on SDS-polyacrylamide gel (Fig. 3*B*). More than 40 ng of irreversibly hyperoxidized Tsa1p was detectable with anti-Tsa1p-SO_3H antiserum in a dose-dependent manner, whereas 100 ng of reversibly hyperoxidized Tsa1p was not detectable (Fig. 3, *B* and *C*).

Mass Analysis of Irreversibly Hyperoxidized Tsa1p—The mass of irreversibly hyperoxidized Tsa1p was determined by electrospray ionization mass spectrometry. Irreversibly hyperoxidized Tsa1p was purified from crude extracts of yeast cells treated with 10 mM hydrogen peroxide as described previously for the purification of Tsa1p-SH (39). Irreversibly hyperoxidized Tsa1p was identified by SDS-PAGE and two-dimensional PAGE analyses (Fig. 4, *A* and *B*). The mass spectra of reduced Tsa1p and irreversibly hyperoxidized Tsa1p with multiple charges are shown in Fig. 4*C*. The calculated monoisotopic mass values were 21,458.4 and 21,506.2 Da, respectively. The mass difference was ~48 Da, which suggests the presence of three oxygen atoms in irreversibly hyperoxidized Tsa1p. Considering the reactivity to anti-Tsa1p-SO_3H antiserum, the site of oxidation is the C_P residue, and thus, irreversibly hyperoxidized Tsa1p is certainly a Tsa1p-C_P-SO_3H.

Tsa1p-SO_3H Is Not a Spontaneous Oxidation Product of Tsa1p-SO_2H—Previous reports proposed the autoxidation of protein cysteine sulfinic acid to cysteine sulfonic acid at the peptide level (40–42) and the protein level (43) in the presence of dissolved oxygen. We examined whether Tsa1p-SO_2H resulted in spontaneous oxidation to Tsa1p-SO_3H in crude cell lysates and an *in vitro* system. Yeast cell lysate treated with 0.5 mM hydrogen peroxide for 10 min was exposed to air for 5 days at 4 °C without a reducing agent. Initially, about half of the Tsa1p was hyperoxidized to Tsa1p-SO_2H based on the retroreducibility (Fig. 5*A*) and the negligible reactivity to anti-Tsa1p-SO_3H antiserum (Fig. 5*B*). At up to 5 days of air exposure, neither a change in the ratio of reduced to hyperoxidized forms nor a change in the reactivity to anti-Tsa1p-SO_3H antiserum was observed (Fig. 5*B*). Purified Tsa1p-SO_2H showed consistent results (Fig. 5*D*). Atmospheric oxygen was not capable of further oxidizing Tsa1p-SO_2H even under denaturing conditions in the presence of 6 M guanidine HCl (Fig. 5, *B* and *D*, *middle panels*). In addition, pH increases up to 8.5 with 6 M guanidine HCl did not cause the autoxidation of Tsa1p-SO_2H to Tsa1p-SO_3H, and the yeast culture and storage conditions also did not cause the autoxidation of Tsa1p-SO_2H (data not shown).

Maintenance of Tsa1p-SO_3H in Cells—Irreversibly oxidized proteins in cells are generally believed to be degraded by proteolytic systems employing principally the 20 S proteasome as well as the ubiquitin-26 S proteasome pathways (35, 36). To examine the life span of Tsa1p-SO_3H in yeast cells, exponentially growing yeast cells were exposed to 10 mM hydrogen per-

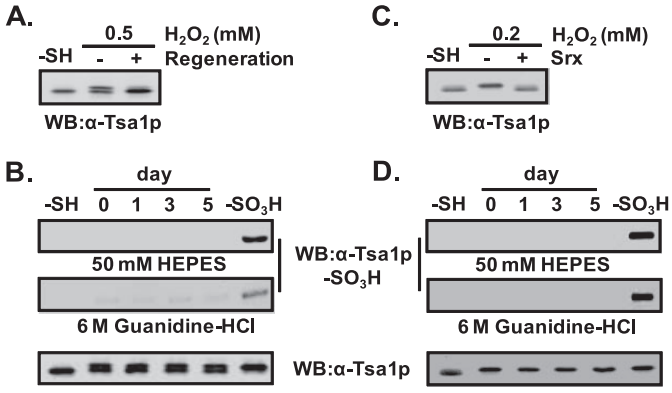

FIGURE 5. **Tsa1p-SO_3H is not an autoxidation product of Tsa1p-SO_2H.** *A*, for the preparation of Tsa1p-SO_2H, yeast cells were exposed to 0.5 mM H_2O_2 at 30 °C for 10 min and then incubated for 3 h in fresh SD medium in the presence of 50 μg/ml cycloheximide to confirm the reversibility of hyperoxidized Tsa1p. *B*, after exposure to 0.5 mM H_2O_2 for 10 min at A_{600} = 0.5, the lysates were prepared in 50 mM HEPES-NaOH (pH 7.0) containing 1 mM EDTA and 1 mM phenylmethylsulfonyl fluoride. Crude lysates (~4 mg/ml) were diluted to 1 mg/ml with 50 mM HEPES-NaOH (pH 7.0) or 6 M guanidine HCl (final concentration) (pH 8.0) and then subjected to air exposure at 4 °C for 5 days. Samples were taken at the indicated time points, and autoxidation to Tsa1p-SO_3H was analyzed by immunoblotting with anti-Tsa1p-SO_3H antibody. *C*, Tsa1p-SO_2H was prepared from purified Tsa1p-SH (0.3 μM) by treatment with 0.2 mM H_2O_2 in the presence of a Trx-dependent oxidation mixture containing 50 mM HEPES-NaOH (pH 7.0), 5.95 μM Trx, 0.1 μM Trx reductase, and 0.25 mM NADPH for 10 min at 30 °C. Oxidation to Tsa1p-SO_2H was confirmed by retroreduction in a mixture containing 1.2 μM Srx1, 1 mM ATP, 1 mM $MgCl_2$, and 2.5 mM DTT for 1 h at 30 °C. *D*, autoxidation of purified Tsa1p-SO_2H to Tsa1p-SO_3H was performed as described for *B*. *WB*, Western blot.

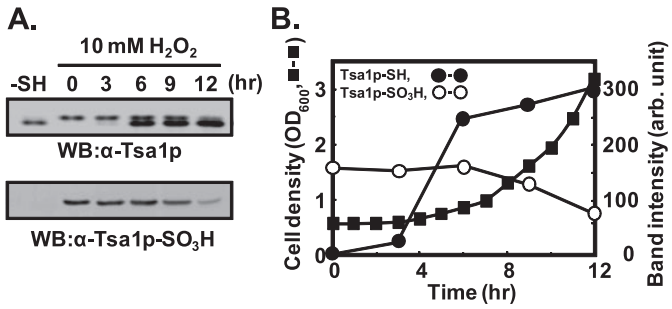

FIGURE 6. **Maintenance of Tsa1p-SO_3H in growing yeast cells.** *A*, log-phase yeast cells (A_{600} = 0.5) were exposed to 10 mM H_2O_2 and then incubated with fresh SD medium at 30 °C. At the indicated time points, yeast cells in 30 ml of culture were collected and disrupted. The same volume of each sample was separated on 12% SDS-polyacrylamide gel followed by immunoblotting with anti-Tsa1p and anti-Tsa1p-SO_3H antibodies. *WB*, Western blot. *B*, growth of yeast cells in fresh SD medium after H_2O_2 exposure was monitored by absorbance at 600 nm (■). The relative amounts of Tsa1p-SO_3H (○) and Tsa1p-SH (●) Western immunoblot bands were quantified from the immunoblot (*A*, *upper panel*) by densitometry (Gel Doc XR system, Bio-Rad). *arb.*, arbitrary.

oxide for 10 min and incubated with fresh SD medium. After 4 h of lag phase, yeast cells achieved exponential growth with a doubling time of ~3 h (Fig. 6*B*). The Tsa1p-SO_3H level did not change much until 6 h and then gradually decreased. From 6 to 12 h of the culture period, the cell number doubled twice, whereas total Tsa1p-SO_3H decreased to half of the initial level. Because of the long lag period after the treatment with hydrogen peroxide, the determination of the half-life of Tsa1p-SO_3H in yeast cells might be controversial. If we define the Tsa1p-SO_3H half-life in exponentially growing yeast cells, it is reasonably estimated to be 6 h (Fig. 6). The negligible rate of irreversible hyperoxidation of Tsa1p under normal culture conditions and the maintenance of Tsa1p-SO_3H over more than two doubling periods implicate a new role for Tsa1p-SO_3H in yeast cells rather than overoxidized protein wastes.

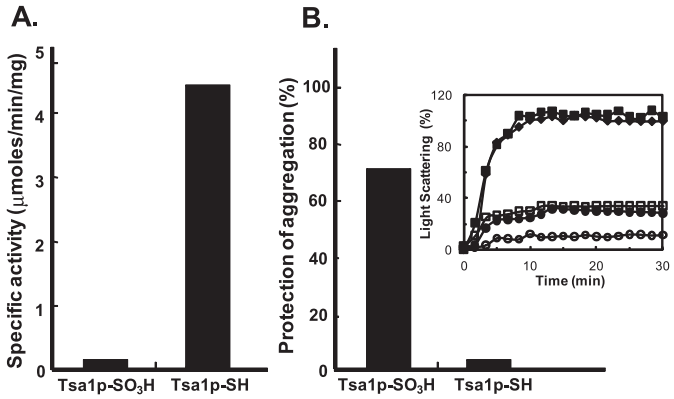

FIGURE 7. **Switch from a peroxidase to an enhanced molecular chaperone by hyperoxidation.** *A*, the rate of peroxide reduction was determined as described previously (13) with 0.3 μM purified Tsa1p-SH or Tsa1p-SO_3H in a 150-μl reaction mixture. *B*, the molecular chaperone activity was measured using luciferase as a substrate. Luciferase (0.15 μM) was incubated with Tsa1p-SH or Tsa1p-SO_3H in the indicated ratios in 25 mM HEPES-KOH buffer (pH 7.9) at 47 °C for 30 min, and substrate aggregation was monitored by measuring the light scattering at 320 nm. The relative capacities of protection against aggregation at a molar ratio of 0.5:1 (Tsa1p/luciferase) were compared. The assay mixture before heating was set to 100% protection against aggregation. *Inset*, control luciferase (♦), 2:1 Tsa1p-SH/luciferase (●), 0.5:1 Tsa1p-SH/luciferase (■), 2:1 Tsa1p-SO_3H/luciferase (○), and 0.5:1 Tsa1p-SO_3H/luciferase (□). The aggregation rate of control luciferase at 30 min was set to 100%.

Loss and Gain of Catalytic Activity by Hyperoxidation—Trx-dependent peroxidase activity was lost by hyperoxidation at C_P (Fig. 7*A*), but the considerable maintenance of Tsa1p-SO_3H in the yeast cells led us to explore the endogenous catalytic activity of Tsa1p-SO_3H. We measured the molecular chaperone activity of Tsa1p-SO_3H because the oligomeric structure-dependent functional switching of Tsa1p from a peroxidase to a molecular chaperone and vice versa has been reported (31). Chaperone activities were determined by measuring the protection capacity of the heat-induced aggregation of luciferase. The molar ratios of Tsa1p-SH and Tsa1p-SO_3H to luciferase requiring 70% protection were 2:1 and 0.5:1, respectively. Thus, Tsa1p-SO_3H had ~4-fold higher chaperone activity compared with Tsa1p-SH (Fig. 7*B*).

Oligomeric Structure of Tsa1p-SO_3H—The correlation between chaperone activities and their structures has been established in many small heat shock proteins (19, 29, 44). We explored whether this correlation is also applicable to Tsa1p-SO_3H. A functional switching of Tsa1p from a peroxidase to a molecular chaperone accompanied by a shift to a higher molecular mass complex has been observed (31–33). Purified Tsa1p-SH from yeast cells was separated into two major peaks on a size exclusion chromatography column (TSK-GEL G3000SWXL) with calculated molecular masses of ~600 and 40 kDa, corresponding to two dodecameric forms and a dimeric form. Tsa1p-SO_3H eluted with one major peak at ~530 kDa, which we suppose to be two dodecamers (Fig. 8*A*). To compare the oligomeric structures of Tsa1p-SH and Tsa1p-SO_3H, we performed electron microscopy, and the proteins were visualized by negative staining with uranyl acetate. Tsa1p-SO_3H showed a homogeneous ring-shaped structure 14 nm in diameter, whereas Tsa1p-SH showed an irregular configuration with

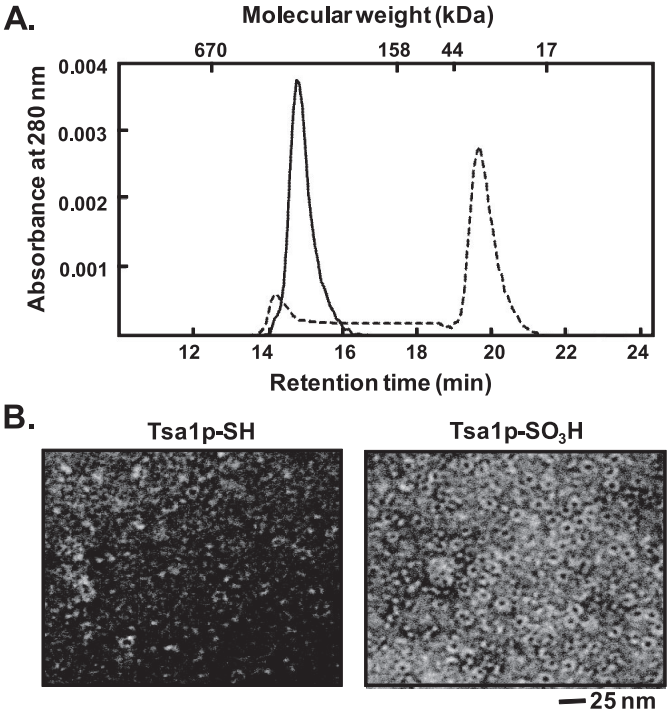

FIGURE 8. **Structure analysis of Tsa1p-SH and Tsa1p-SO_3H by size exclusion chromatography and electron microscopy.** *A*, 10 μg of purified Tsa1p-SH (*dashed line*) and 10 μg of Tsa1p-SO_3H (*straight line*) were separated on a TSK-GEL G3000SWXL column equilibrated with 50 mM sodium phosphate (pH 7.0) and 0.1 M NaCl. *B*, the electron micrographs of Tsa1p-SH and Tsa1p-SO_3H were obtained by negative staining with 2% uranyl acetate.

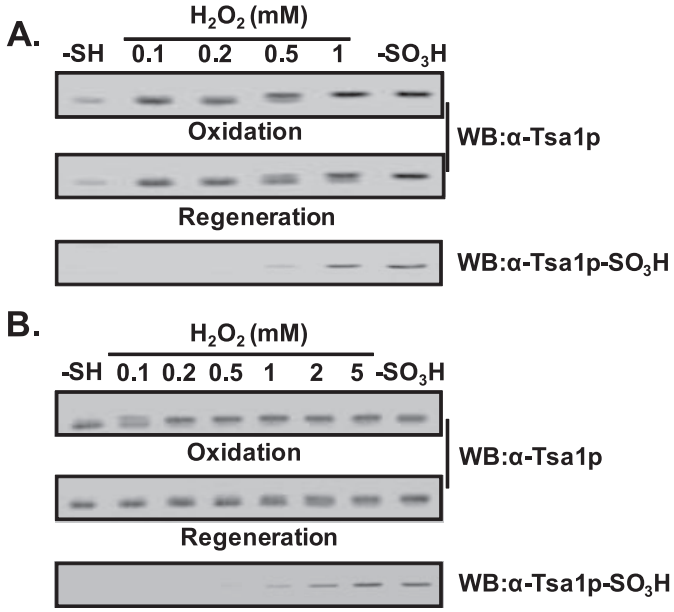

FIGURE 9. **Sulfonic hyperoxidation of Tsa1p in yeast cells and *in vitro*.** *A*, exponentially growing yeast cells (6×10^6) were treated with the indicated concentrations of H_2O_2 for 10 min. The oxidation states of Tsa1p were determined by immunoblotting with anti-Tsa1p-SO_3H antibody. The retroreduction assay was performed in 50 mM HEPES-NaOH (pH 7.0) containing cell lysates (50 μg of crude extract), 1.2 μM Srx1, 1 mM ATP, 1 mM $MgCl_2$, and 2.5 mM DTT for 1 h at 30 °C. *B*, purified Tsa1p-SH (0.3 μM) was oxidized with various concentrations of H_2O_2 in a Trx-dependent oxidation system containing 5.95 μM Trx, 0.1 μM Trx reductase, and 0.25 mM NADPH. The regeneration assay was performed as described for *A*. For the quantitative evaluation of the protein bands, 8 and 30 ng of Tsa1p-SO_3H were used as standards for the detection with anti-Tsa1p and anti-Tsa1p-SO_3H antisera, respectively. *WB*, Western blot.

~10% of a sporadic ring-shaped structure (Fig. 8*B*). Sphere-shaped particles were not found with either Tsa1p-SH or Tsa1p-SO_3H. These results confirm that irreversible hyperoxidation induces oligomerization to higher molecular mass forms, which we suppose to be two dodecamers, and that these higher molecular mass structures are responsible for a molecular chaperone function.

Comparison of Sulfonyl Hyperoxidation in Yeast Cells and an in Vitro System—In vitro preparation of Tsa1p-SO_2H using the Trx system was feasible, and the hyperoxidized product was mostly Tsa1p-SO_2H (Figs. 3 and 5). In contrast, preparation of Tsa1p-SO_2H using yeast cells was not successful because the hyperoxidized products were a mixture of Tsa1p-SO_2H and Tsa1p-SO_3H (data not shown). In addition, preparation of Tsa1p-SO_3H in an *in vitro* system was also feasible (Fig. 3); however, conditions harsher than those used with yeast cells were usually required. Because of this discrepancy, we compared the sulfonyl hyperoxidation in both systems more precisely. Most of the Tsa1p was hyperoxidized to Tsa1p-SO_2H upon treatment with 0.2 mM hydrogen peroxide in the *in vitro* system, whereas most of the Tsa1p in yeast cells was not hyperoxidized under the same conditions. Although the Tsa1p in both systems was hyperoxidized by 1 mM hydrogen peroxide, the principal form in yeast cells was Tsa1p-SO_3H, whereas in the *in vitro* system, it was Tsa1p-SO_2H (Fig. 9). Considered an effective intrinsic antioxidant system in yeast cells, the hydrogen peroxide concentration that Tsa1p must cope with in yeast cells should be much lower than in the *in vitro* system. The more feasible sulfonyl hyperoxidation in yeast cells suggests the possible existence of a facilitation system other than the Trx system for the reaction from Tsa1p-SH to Tsa1p-SO_3H or from Tsa1p-SO_2H to Tsa1p-SO_3H in yeast cells.

DISCUSSION

In contrast to catalases, which directly catalyze the decomposition of peroxides to water and oxygen, peroxidases, which consume expensive cellular reducing equivalents to reduce peroxides, should be systematically regulated to conserve cellular reducing resources. After the finding of inactivation of Tsa1p during peroxidase catalysis in yeast (13), the hyperoxidation of active-site cysteine (C_P) from sulfhydryl to sulfinic or sulfonic acid in *in vitro* assays and in-cell analysis was reported (14–17). In addition, studies that followed reported the reversibility of sulfinic C_P to sulfhydryl in mammalian 2-Cys Prxs and enzymatic systems responsible for that retroreduction in yeast and mammalian systems (25–28).

To quantify hyperoxidized Tsa1p in yeast cells using immunological methods, we developed rabbit antiserum against the peptide encompassing Tsa1p-C_P-SO_3H using the same method as described previously for mammalian anti-Prx-SO_3H antiserum (38). We identified two different forms of hyperoxidized Tsa1p (reversible Tsa1p-SO_2H and irreversible Tsa1p-SO_3H) (Figs. 1–4) based on the reactivity of the antiserum we developed. In contrast to mammalian anti-Prx-SO_3H antiserum, which equally recognizes both Prx-C_P-SO_2H and Prx-C_P-SO_3H (38), the reactivity of anti-Tsa1p-SO_3H antiserum was specific to Tsa1p-C_P-SO_3H (Fig. 3). Tsa1p-C_P-SO_3H was detectable

above 20 ng in our alkaline phosphatase-based immune complex detection system, but 100 ng of Tsa1p-SO_2H was not visible using the same detection system (Fig. 3). When HeLa cell extracts treated with various concentrations of hydrogen peroxide were probed, anti-Tsa1p-SO_3H antiserum clearly showed distinguishable reactivity toward irreversibly hyperoxidized 2-Cys Prx spots, although the exact oxidation status of C_P needs to be verified (data not shown). Considering the active-site amino acid sequence identity between yeast Tsa1p (-AFTFV**C_P**PTEI-) and mammalian 2-Cys Prx (-DFTFV**C_P**PTEI-), anti-Tsa1p-SO_3H antiserum can also be used for the detection of mammalian irreversibly hyperoxidized 2-Cys Prx proteins. The points that Tsa1p-SO_3H has a half-life of more than two doubling times in yeast, Tsa1p-SO_3H is not an autoxidation product, and Tsa1p-SO_3H is an irreversibly hyperoxidized product together support the use of Tsa1p-SO_3H as a molecular marker of cumulative oxidative stress in cells. Anti-Tsa1p-SO_3H antiserum, which specifically recognizes irreversibly hyperoxidized Tsa1p as well as mammalian 2-Cys Prxs, can be an efficient tool for probing a cell's history of withstanding oxidative stresses.

Once impaired by oxidative stress, proteins are generally considered cellular waste and designated for degradation by the proteasome in cells. The longer half-life of irreversibly hyperoxidized Tsa1p-SO_3H (Fig. 6) compared with the average half-life of yeast proteins (37) suggests an intrinsic role for hyperoxidized Tsa1p-SO_3H in oxidatively stressed yeast cells. We identified the enhanced molecular chaperone activity and corresponding oligomeric structure of Tsa1p-SO_3H (Figs. 7 and 8). Tsa1p-SO_3H functioning as a molecular chaperone in cells is considered to be an advantage over Tsa1p-SH or Tsa1p-SO_2H in cells. Presumably, Tsa1p-SO_2H has a considerably shorter life span than Tsa1p-SO_3H because most of the Tsa1p-SO_2H is retroreduced to Tsa1p-SH when Srx1 is available. Because Srx1 is a noticeably inefficient enzyme with a very low turnover rate (k_{cat} = 0.1–0.8/min) (28) and because proper oligomeric structure is responsible for chaperone function, Tsa1p-SO_2H seems likely to act as a molecular chaperone only briefly until association with Srx1 for retroreduction. Tsa1p-SH has several different oligomeric forms (Fig. 8*B*) (31), which is the reason why it is a less effective molecular chaperone than Tsa1p-SO_3H. Therefore, Tsa1p-SO_3H functions as the most effective and longest lived molecular chaperone among the Tsa1p redox forms in yeast cells.

Comparing Tsa1p hyperoxidation in yeast cells with that in an *in vitro* oxidation system, we found that reversible sulfinyl hyperoxidation was the favored reaction in the *in vitro* system but not in the yeast cells. In contrast, irreversible sulfonyl hyperoxidation was preferred in yeast cells (Fig. 9). Our results show that atmospheric oxygen is not capable of oxidation of Tsa1p-SO_2H to Tsa1p-SO_3H (Fig. 5), which is consistent with previous observations (40–43). Hyperoxidation *in vitro* takes place only during peroxidatic turnover in the presence of a recycling system including Trx, Trx reductase, and NADPH (17). Taken together, the *in vitro* preference of sulfinyl hyperoxidation and the *in vivo* preference of sulfonyl hyperoxidation suggest the possible existence of an enzymatic system other than the Trx system that facilitates sulfonyl hyperoxidation in yeast cells, and it remains to be elucidated. In summary, we have identified Tsa1p-SO_3H and its function as an effective and stable molecular chaperone and as a cellular marker that retains a cell's cumulative index of oxidative stress.

REFERENCES

1. Rhee, S. G. (2006) *Science* **312,** 1882–1883
2. Jabob, C., Knight, I., and Winyard, P. G. (2006) *Biol. Chem.* **387,** 1385–1397
3. Cross, J. V., and Templeton, D. J. (2006) *Antioxid. Redox Signal.* **8,** 1819–1827
4. Barford, D. (2004) *Curr. Opin. Struct. Biol.* **14,** 679–686
5. Jacob, C., Giles, G. I., Giles, N. M., and Sies, H. (2003) *Angew. Chem. Int. Ed. Engl.* **42,** 4742–4758
6. Kiley, P. J., and Storz, G. (2004) *PLos Biol.* **2,** 1714–1717
7. Poole, L. B., Karplus, P. A., and Claiborne, A. (2004) *Pharmacol. Toxicol.* **44,** 325–347
8. Jacob, C., Holme, A. L., and Fry, F. H. (2004) *Org. Biomol. Chem.* **2,** 1953–1956
9. Rhee, S. G., Chae, H. Z., and Kim, K. (2005) *Free Radic. Biol. Med.* **38,** 1543–1552
10. Poole, L. B. (2005) *Arch. Biochem. Biophys.* **433,** 240–254
11. Wood, Z. A., Schröder, E., Robin Harris, J., and Poole, L. B. (2003) *Trends Biochem. Sci.* **28,** 32–40
12. Hofmann, B., Hecht, H. J., and Flohe, L. (2002) *Biol. Chem.* **383,** 347–364
13. Chae, H. Z., Chung, S. J., and Rhee, S. G. (1994) *J. Biol. Chem.* **269,** 27670–27678
14. Mitsumoto, A., Takanezawa, Y., Okawa, K., Iwamatsu, A., and Nakagewa, Y. (2001) *Free Radic. Biol. Med.* **30,** 625–635
15. Rabilloud, T., Heller, M., Gasnier, F., Luche, S., Rey, C., Aebersold, R., Benahmed, M., Louisot, P., and Lunardi, J. (2002) *J. Biol. Chem.* **277,** 19396–19401
16. Wagner, E., Luche, S., Penna, L., Chevallet, M., Dorsselaer, A. V., Leize-Wagner, E., and Rabilloud, T. (2002) *Biochem. J.* **366,** 777–785
17. Yang, K. S., Kang, S. W., Woo, H. A., Hwang, S. C., Chae, H. Z., Kim, K., and Rhee, S. G. (2002) *J. Biol. Chem.* **277,** 38029–38036
18. Fu, X., Kassim, S. Y., Parks, W. C., and Heinecke, J. W. (2001) *J. Biol. Chem.* **276,** 41279–41287
19. Haslbeck, M., Franzmann, T., Weinfurtner, D., and Buchner, J. (2005) *Nat. Struct. Mol. Biol.* **12,** 842–846
20. Kinumi, T., Kimata, J., Taira, T., Ariga, H., and Niki, E. (2004) *Biochem. Biophys. Res. Commun.* **317,** 722–728
21. Mallis, R. J., Hamann, M. J., Zhao, W., Zhang, T., Hendirch, S., and Thomas, J. A. (2002) *Biol. Chem.* **383,** 649–662
22. Seth, D., and Rudolph, H. (2006) *Biochemistry* **45,** 8476–8487
23. Salmeen, A., Andersen, J. N., Myers, M. P., Meng, T. C., Hinks, J. A., Tonks, N. K., and Barford, D. (2003) *Nature* **432,** 769–773
24. van Montfort, R. L., Conqreve, M., Tisi, D., Carr, R., and Jhoti, H. (2003) *Nature* **423,** 773–777
25. Woo, H. A., Chae, H. Z., Hwang, S. C., Yang, K. S., Kang, S. W., Kim, K., and Rhee, S. G. (2003) *Science* **300,** 592–594
26. Biteau, B., Labarre, J., and Toledano, M. B. (2003) *Nature* **425,** 980–984
27. Budanov, A. V., Sablina, A. A., Feinstein, E., Koonin, E. V., and Chumakov, P. M. (2004) *Science* **304,** 596–600
28. Chang, T.-S., Jeong, W., Woo, H. A., Lee, S. M., Park, S., and Rhee, S. G. (2004) *J. Biol. Chem.* **279,** 50994–51001
29. Nakamoto, H., and Vigh, L. (2007) *CMLS Cell. Mol. Life Sci.* **64,** 294–306
30. Vivancos, A. P., Castillo, E. A., Biteau, B., Nicot, C., Ayté, J., Toledano, M. B., and Hidalgo, E. (2005) *Proc. Natl. Acad. Sci. U. S. A.* **201,** 8875–8880
31. Jang, H. H., Lee, K. O., Chi, Y. H., Jung, B. G., Park, S. K., Park, J. H., Lee, J. R., Lee, S. S., Moon, J. C., Yun, J. W., Choi, Y. O., Kim, W. Y., Kang, J. S., Cheong, G. W., Yun, D. J., Rhee, S. G., Cho, M. J., and Lee, S. Y. (2004) *Cell* **117,** 625–635
32. Rhee, S. G., Jeong, W., Chang, T.-S., and Woo, H. A. (2007) *Kidney Int.* **106,** (suppl.) S3–S8
33. Moon, J. C., Hah, Y. S., Kim, W. Y., Jung, B. G., Jang, H. H., Lee, J. R., Kim, S. Y., Lee, Y. M., Jeon, M. G., Kim, C. W., Cho, M. J., and Lee, S. Y. (2005)

J. Biol. Chem. **280,** 28775–28784
34. Phalen, T. J., Weirather, K., Deming, P. B., Anathy, V., Howe, A. K., van der Vliet, A., Jönsson, T. J., Poole, L. B., and Heintz, N. H. (2006) *J. Cell Biol.* **175,** 779–789
35. Friguet, B. (2006) *FEBS Lett.* **580,** 2910–2916
36. Stadtman, E. R. (2006) *Free Radic. Res.* **40,** 1250–1258
37. Belle, A., Tanay, A., Bitincka, L., Shamir, R., and O'Shea, E. K. (2006) *Proc. Natl. Acad. Sci. U. S. A.* **103,** 13004–13009
38. Woo, H. A., Kang, S. W., Kim, H. K., Yang, K. S., Chae, H. Z., and Rhee, S. G. (2003) *J. Biol. Chem.* **278,** 47361–47364
39. Kim, K., Kim, I. H., Lee, K. Y., Rhee, S. G., and Stadtman, E. R. (1988) *J. Biol. Chem.* **263,** 4704–4711
40. Poole, L. B., and Claiborne, A. (1989) *J. Biol. Chem.* **264,** 12330–12338
41. Kice, J. L. (1980) *Adv. Phys. Org. Chem.* **17,** 65–181
42. Hayward, M. A., Campbell, E. B., and Griffith, O. W. (1987) *Methods Enzymol.* **143,** 279–281
43. Fujiwara, N., Nakano, M., Kato, S., Yoshihara, D., Ookawara, T., Eguchi, H., Taniguchi, N., and Suzuki, K. (2007) *J. Biol. Chem.* **282,** 35933–35944
44. Sun, Y., and MacRae, T. H. (2005) *CMLS Cell. Mol. Life Sci.* **62,** 2460–2476

Irreversible Oxidation of the Active-site Cysteine of Peroxiredoxin to Cysteine Sulfonic Acid for Enhanced Molecular Chaperone Activity

Jung Chae Lim, Hoon-In Choi, Yu Sun Park, Hyung Wook Nam, Hyun Ae Woo, Ki-Sun Kwon, Yu Sam Kim, Sue Goo Rhee, Kanghwa Kim and Ho Zoon Chae

J. Biol. Chem. 2008, 283:28873-28880.
doi: 10.1074/jbc.M804087200 originally published online August 25, 2008
